9690 *Macromolecules* **2010**, *43*, 9690–9697
DOI: 10.1021/ma1021264

Macromolecules
ARTICLE

Mannose-Substituted Conjugated Polyelectrolyte and Oligomer as an Intelligent Energy Transfer Pair for Label-Free Visual Detection of Concanavalin A

Kan-Yi Pu,[†] Jianbing Shi,[†,‡] Lihua Wang,[†,§] Liping Cai,[†] Guan Wang,[†] and Bin Liu*[,†]

[†]*Department of Chemical and Biomolecular Engineering, 4 Engineering Drive 4, National University of Singapore, Singapore 117576, Singapore,* [‡]*College of Materials Science and Engineering, Beijing Institute of Technology, Beijing 100081, China, and* [§]*Laboratory of Physical Biology, Shanghai Institute of Applied Physics, Chinese Academy of Sciences, Shanghai 201800, China*

Received September 14, 2010; Revised Manuscript Received November 1, 2010

ABSTRACT: Mannose-substituted blue-fluorescent cationic conjugated polyelectrolyte (**P1**) and yellow-fluorescent neutral conjugated oligomer (**6**) are synthesized via the combination of Suzuki coupling polymerization and click chemistry. The spectral overlap between the emission of **P1** and the absorption of **6** allows one to blend them to form an intelligent fluorescence resonance energy transfer (FRET) pair for multicolor protein sensing. Despite the nonspecific-interaction-induced perturbation in the polymer emission, strong specific binding between mannose and Concanavalin A (ConA) is able to result in protein-selective FRET from **P1** to **6**. The fluorescence of **6**/**P1** blend in the presence of ConA is dominated by yellow emission, while it remains blue in the presence of other six nonspecific proteins. The **6**/**P1** blend thus serves as a multicolor bicomponent FRET probe for label-free visual detection of ConA in a high-contrast and convenient manner. In addition, its linear ratiometric fluorescence response toward ConA enables effective protein quantification with a low limit of detection of ~1.5 nM. This study demonstrates the importance of molecular engineering in conjugated polyelectrolyte based label-free chemical and biological sensing.

Introduction

Reliable technologies for efficient and convenient protein detection are of scientific importance and economic interest due to their vital implications in proteomics, medical diagnostics, and pathogen detection.[1] The structural complexity and environmental sensitivity of proteins relative to other biomolecules necessitate extra severe considerations for the sensory design.[2] Challenges in protein sensing primarily lie on the creation of sensory materials not only featuring appropriate receptors for efficient binding with target proteins but also bearing perturbable functionalities for sensitive transduction of recognition events. In this regard, conjugated polyelectrolytes (CPEs) comprising π-conjugated fluorescent backbones with amenable water-soluble side chains well meet these criteria, providing a unique optical platform for protein sensing.[3] In particular, their large absorption extinction coefficients and rapid intramolecular/intermolecular exciton migration make CPEs light-harvesting antennae in optical transduction, ultimately imparting amplified signals and improved sensitivity relative to traditional small fluorophores.[4]

Protein detection based on fluorescent, colorimetric, or fluorescence resonance energy transfer (FRET) properties of CPEs has been reported. Fluorescence quenching of CPEs toward proteins via electron transfer or polymer aggregation mechanism enabled array-based protein discrimination according to the pattern of Stern−Volmer quenching constants;[5] whereas, conformation-dependent absorption behaviors of cationic polythiophene (PT) in association with strong aptamer/protein binding allowed for specific colorimetric recognition of human thrombin.[6] In addition, distance-dependent FRET between CPEs and dye-labeled biomolecules led to both array-based[7] and specific protein assays.[8] In comparison with fluorescence quenching and colorimetric protocols, FRET strategy has the advantage of dual-channel signal collection, consequently giving rise to reduced possibility of false-positive signals.[9] However, since biomolecular labeling is laborious and complicated,[10] the requirement of dye-labeled biomolecules to participate in FRET sensing strongly constrains the assay applications. As a result, development of CPEs as label-free FRET probes for protein sensing is highly desirable.

We are particularly interested in developing CPEs with energy donor−acceptor backbones for chemical and biological detection.[11] Recently, we synthesized a series of anionic polyfluorene (PF) derivatives containing different fractions of long-wavelength emissive 2,1,3-benzothiadiazole (BT) units to show multicolor responses toward proteins.[11c] The working hypothesis is that interchain FRET is more efficient than intrachain FRET because of stronger electronic coupling and increased energy transfer dimensionality for interchain vs intrachain interactions.[12] Polymer aggregation concurs with CPE/protein complexation to favor both intrachain and interchain FRET from the donor segments to the acceptor units, leading to fluorescent color changes. However, as the fluorescent signals are mainly determined by nonspecific hydrophobic and electrostatic interactions between the polymer and proteins,[13] these probes suffer from low signal-to-noise ratio and poor selectivity. To overcome this limitation, recognition groups were covalently attached to BT-containing polymers as the side chains in an attempt to bring specific polymer/protein binding into sensing operation.[11g] Unfortunately, the specific binding failed to significantly outperform nonspecific interference to dominate the fluorescence signatures. The above information reveals that single-component FRET systems generated from incorporation of low-energy units into CPEs can not provide very effective protein detection, which

*To whom correspondence should be addressed. Fax: (+65) 6779-1936. E-mail: cheliub@nus.edu.sg.

 Published on Web 11/12/2010

Scheme 1. Chemical Structures of P1 and 6

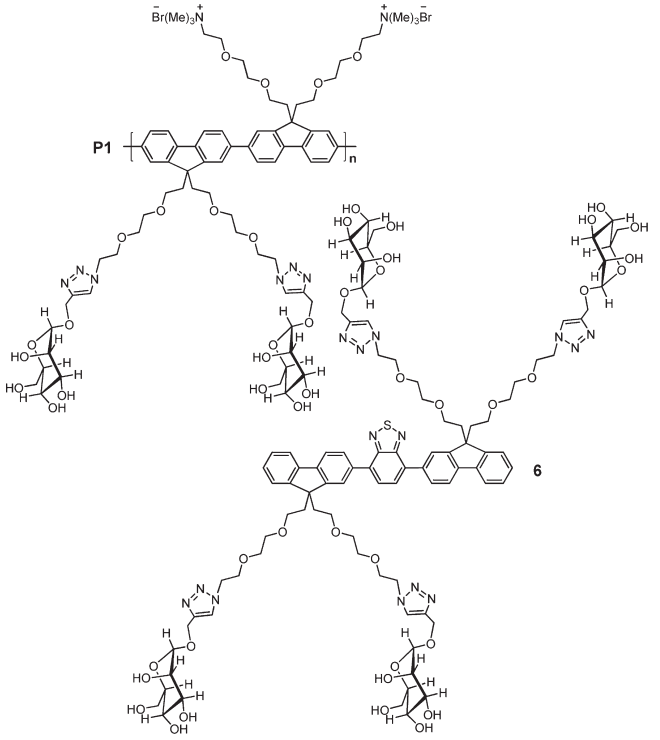

intrinsically stems from the strong hydrophobic and charged nature of both CPEs and proteins.

In this contribution, we report that a CPE and a neutral conjugated oligomer can serve as an intelligent bicomponent FRET probe for highly selective label-free protein sensing. To demonstrate this concept, Concanavalin A (ConA) is chosen as the target protein herein, which is a lectin protein that plays a crucial role in cell signaling, cell surface recognition, and pathogen docking.[14] Considering the high affinity between mannose and ConA,[15] both PF-based energy-donating CPE (**P1**) and BT-based energy-accepting conjugated oligomer (**6**) are endowed with mannose as the recognition groups (chemical structures shown in Scheme 1). As conjugated polymers fully substituted with mannose groups are hard to be dissolved in aqueous solution,[16] half of the side chains of **P1** is designed to have charges in order to maintain water solubility. By virtue of its short hydrophobic aromatic backbone and nonionic nature, **6** should have weak interactions with nonspecific proteins. As such, FRET between **P1** and **6** is anticipated to selectively occur in the presence of ConA, leading to label-free visual detection of ConA.

Results and Discussion

Synthesis and Characterization. A postfunctionalization strategy based on click chemistry was adopted to synthesize mannose-substituted conjugated oligomer **6** as shown in Scheme 2. In the first step, 2-(9,9-bis(2-(2-(2-bromoethoxy)ethoxy)ethyl)-fluorenyl)-4,4,5,5-tetramethyl-1,3,2-dioxaborolane (**1**) was synthesized in 85% yield by heating a mixture of 2-bromo-9,9-bis(2-(2-(2-bromoethoxy)ethoxy)ethyl)fluorene and bis-(pinacolao)diborane with KOAc in dioxane at 85 °C for 12 h. This was followed by palladium-mediated Suzuki cross-coupling reaction between **1** and 4,7-dibromobenzothiadiazole (**2**), which led to 4,7-bis(9,9-bis(2-(2-(2-bromoethoxy)-ethoxy)ethyl)fluorenyl)benzothiadiazole (**3**) in 70% yield. Subsequently, treatment of **3** with sodium azide in dimethylformamide (DMF) at room temperature gave 4,7-bis(9,9-bis(2-(2-(2-azidoethoxy)ethoxy)ethyl)fluorenyl)benzothiadiazole (**4**) in 92% yield. In the last step, CuI-catalyzed click

Scheme 2. Synthesis of Mannose-Substituted Conjugated Oligomer (6)[a]

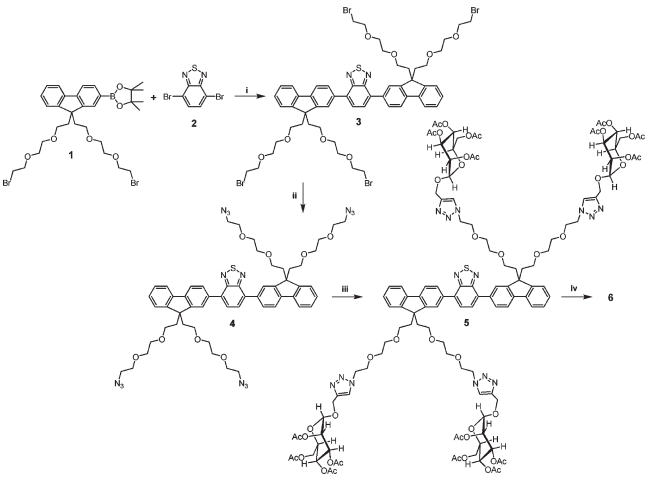

[a] (i) $Pd(PPh_3)_4$, K_2CO_3, H_2O/toluene, 90 °C, 48 h; (ii) NaN_3, DMF, room temperature, 24 h; (iii) 2-propynyl-2,3,4,6-tetra-*O*-acetyl-α-D-mannopyranose, sodium ascorbate, $CuSO_4$, THF/H_2O, room temperature, 24 h; (iv) CH_3ONa, CH_3OH/CH_2Cl_2, room temperature, 6 h.

reaction between **4** and 2-propynyl-2,3,4,6-tetra-*O*-acetyl-α-D-mannopyranose was carried out in tetrahydrofuran (THF)/water at room temperature to afford acetylated precursor **5** in 82% yield. The ^{1}H NMR spectrum of **5** is shown in Figure 1. A single resonance peak of the proton next to the nitrogen atom of the triazole group (−NC*H*=C−, peak *a*) appears at 7.61 ppm, while the triple resonance peak of the methylene protons next to the triazole group (−OCH_2−CH_2−C−, peak *c*) is shifted to 4.42 ppm as compared to that of **4** at 3.44 ppm. Moreover, the single resonance peaks of the acetyl protons are also found at 2.13, 2.10, 2.02, and 1.96 ppm, respectively. These characteristic peaks are indicative of successful attachment of acetylated mannose to the fluorene units. After deacetylation of **5** under Zemplém conditions and dialysis purification using a 1.5 kDa molecular weight cutoff dialysis membrane, the mannose-substituted conjugated oligomer **6** was obtained in 87% yield. The disappearance of the resonance peaks of the acetyl protons in the ^{1}H NMR spectrum (Figure S1 in the Supporting Information) of **6** indicates complete deacetylation. The oligomer **6** has a high water-solubility of ∼28 mg/mL, which benefits from its high density of mannose groups and short aromatic backbone.

The CPE (**P1**) with both cationic and mannose side chains was synthesized according to Scheme 3. Treatment of 2,7-dibromo-9,9-bis(2-(2-(2-bromoethoxy)ethoxy)ethyl)fluorene (**7**) with sodium azide in DMF at room temperature gave 9,9-bis(2-(2-(2-azidoethoxy)ethoxy)ethyl)-2,7-dibromofluorene (**8**) in 92% yield. The CuI-catalyzed click reaction between **8** and 2-propynyl-2,3,4,6-tetra-O-acetyl-α-D-mannopyranose led to monomer **9** with acetylated mannose side groups in 87% yield. The dioxaborolane monomer, 2-(9,9-bis(2-(2-(2-methoxyethoxy)ethoxy)ethyl)-7-(4,4,5,5-tetramethyl-1,3,2-dioxaborolan-2-yl)fluorenyl)-4,4,5,5-tetramethyl-1,3,2-dioxaborolane (**10**) was synthesized in 80% yield by heating a mixture of **7** and bis(pinacolao)diborane with KOAc in dioxane at 85 °C for 12 h. The correct structures of monomers **9** and **10** were confirmed by NMR and mass spectrometry. The standard Suzuki cross-coupling mediated polymerization between **9** and **10** provided the neutral precursor **P0** in 78% yield. The number-average molecular weight and polydispersity of **P0** are 13000 and 2.8, respectively,

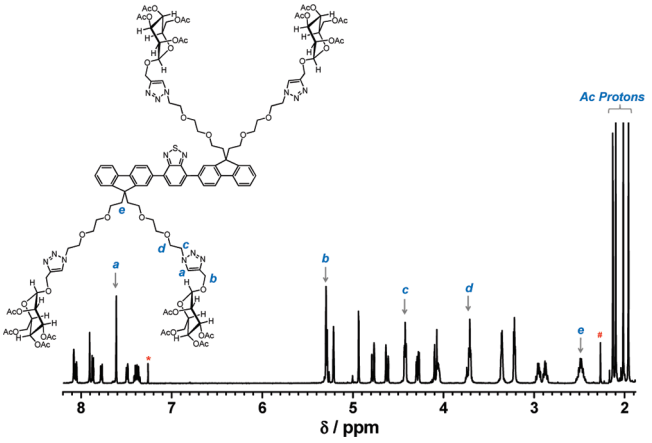

Figure 1. ^{1}H NMR spectrum of **5** in $CDCl_3$. The asterisk and # indicate the peaks of $CDCl_3$ and acetone, respectively.

Scheme 3. Synthesis of Mannose-Substituted CPE (P1) [a]

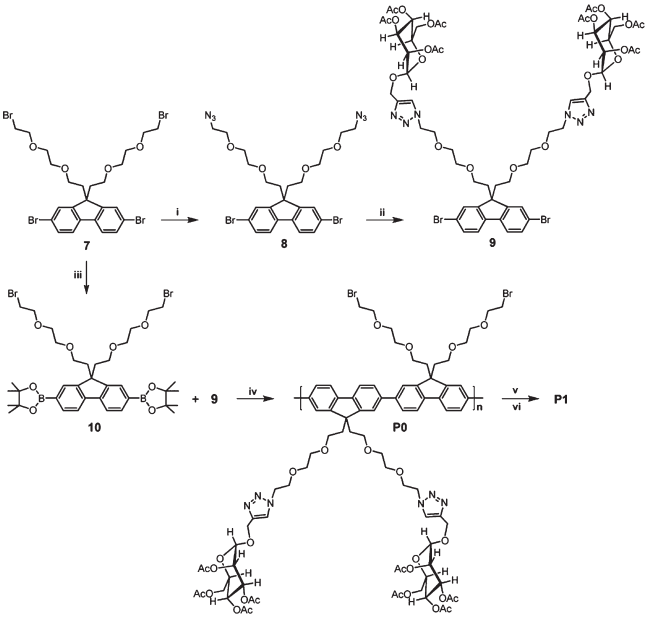

[a] (i) NaN_3, DMF, room temperature, 24 h; (ii) 2-propynyl-2,3,4,6-tetra-*O*-acetyl-α-D-mannopyranose, sodium ascorbate, $CuSO_4$, THF/H_2O, room temperature, 24 h; (iii) bis(pinacolato)diborane, KOAc, [Pd(dppf)Cl_2], anhydrous dioxane, 90 °C; (iv) $Pd(PPh_3)_4$, K_2CO_3, H_2O/toluene, 90 °C, 12 h; (v) CH_3ONa, CH_3OH/CH_2Cl_2, room temperature, 6 h; (vi) $N(CH_3)_3$, THF/CH_3OH, 24 h.

determined by gel permeation chromatography (GPC) using THF as the solvent and polystyrene as the standard. The ^{1}H NMR spectrum of **P0** is shown in Figure 2. The resonance peaks of the methylene protons next to the triazole group ($-NCH_2O-$, peak *a*) and the second-next to the triazole group ($-OCH_2-CH_2-C-$, peak *b*) are located at 5.29 and 3.74 ppm, respectively. The integrated area of each peak is equal to that of the peak at 3.64 ppm corresponding to $-OCH_2-CH_2Br$ (peak *c*). In addition, the characteristic peaks of the acetylated mannose groups are also found. The NMR spectrum indicates the correct chemical structure of **P0**. After deacetylation of **P0** under Zemplém conditions using sodium methylate in methanol/dichloromethane, followed by quaternization with trimethylamine in THF/methanol, **P1** was obtained in 82% yield. The disappearance of the acetyl proton peaks in the ^{1}H NMR spectrum of **P1** indicates complete deacetylation (Figure S2 in the Supporting Information). This polymer was purified by precipitation and dialysis against Mill-Q water using a 6.5 kDa molecular weight cutoff dialysis membrane for 5 days. The water-solubility of **P1** is low (~3 mg/mL), which is due to its long hydrophobic aromatic backbone.

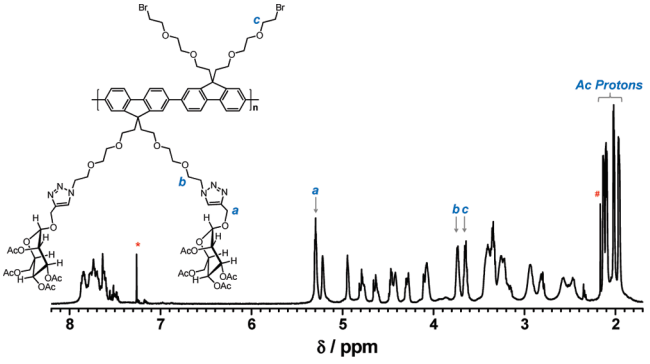

Figure 2. ^{1}H NMR spectrum of **P0** in $CDCl_3$. Asterisk and # indicate the peaks of $CDCl_3$ and acetone, respectively.

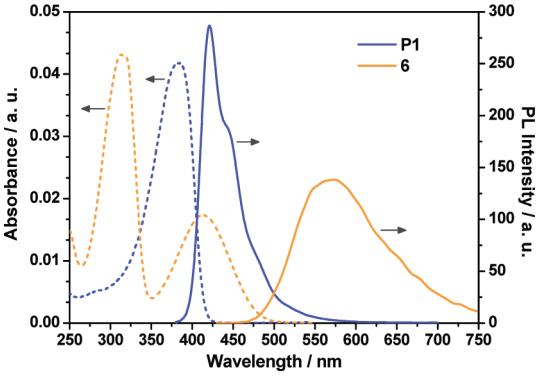

Figure 3. UV−vis absorption (dashed line) and PL (solid line) spectra of **P1** and **6** in water. [**P1 RU**] = 1 μM and [**6**] = 1 μM.

Optical Properties. The UV−vis absorption and photoluminescence (PL) spectra of **P1** and **6** are depicted in Figure 3. The concentration for **P1** based on repeat unit (RU) and **6** based on molecule is 1 μM. The absorption and emission maxima of **P1** are located at 382 and 422 nm, respectively, which are similar to those of water-soluble PF.[17] The absorption spectrum of **6** has two bands centered at 312 and 413 nm, corresponding to fluorene and BT, respectively, while its emission maximum is at 570 nm. The quantum yields of **P1** and **6** in water are 0.55 and 0.32, respectively, measured using quinine sulfate in 0.1 M H_2SO_4 (quantum yield = 0.55) as the standard. The emission spectrum of **P1** well overlaps the absorption spectrum of **6** in the range of 380 to 500 nm, which should favor energy transfer between them for protein sensing.[18]

To optimize the donor/acceptor molar ratio for sensitive optical response toward proteins, the PL spectra of **P1** in the presence of different amount of **6** are examined in 15 mM phosphate buffered saline (PBS, pH = 7.4) containing $CaCl_2$ (0.1 mM) and $MnCl_2$ (0.1 mM) upon excitation at 370 nm. In these experiments, the donor concentration [**P1 RU**] is fixed at 1 μM with the acceptor concentration ([**6**]) varying from 0 to 0.6 μM at intervals of 0.1 μM. As shown in Figure 4, with the increased ratio of [**6**]/[**P1**], the blue emission centered at 422 nm gradually decreases, while the yellow emission band ranging from 518 to 650 nm slightly increases. The spectral change is indicative of weak FRET between **P1** and **6** due to nonspecific interactions. The yellow emission of **6** saturates

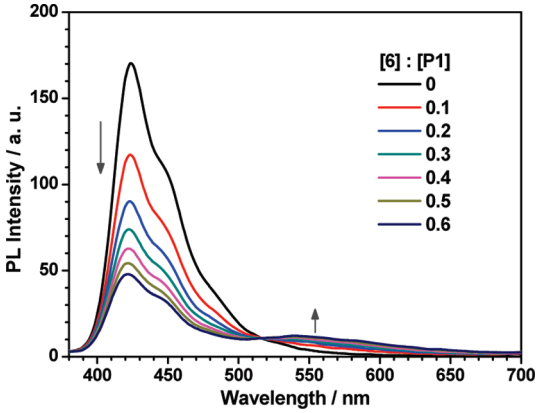

Figure 4. PL spectra of **6**/**P1** blend in 15 mM PBS (pH = 7.4) containing $CaCl_2$ (0.1 mM) and $MnCl_2$ (0.1 mM) with the molar ratio ranging from 0 to 0.6 μM at intervals of 0.1 μM. [**P1 RU**] = 1 μM. Excitation at 370 nm.

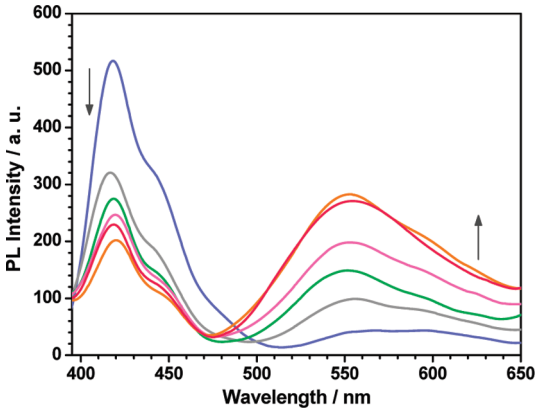

Figure 5. PL spectra of **6**/**P1** blend in PBS (15 mM, pH = 7.2) containing $CaCl_2$ (0.1 mM) and $MnCl_2$ (0.1 mM) in the absence and presence of Con A with the concentration ranging from 0 to 150 nM at intervals of 30 nM. [**P1 RU**] = 1 μM and [**6**] = 0.5 μM. Excitation at 370 nm.

at [**6**]/[**P1**] = 0.5, where the fluorescent color of the blend solution remains blue; whereas, the blue emission of **P1** continues to decrease with further addition of **6**, making the fluorescent color white. As such, the optimum molar ratio of **6** to **P1** for protein sensing is chosen to be 0.5, which represents the highest allowable concentration of **6** to ensure blue background fluorescence.

Protein Sensing. The fluorescence responses of **6**/**P1** blend at the optimal ratio ([**P1 RU**] = 1 μM and [**6**] = 0.5 μM) toward proteins were investigated in PBS buffer (15 mM, pH = 7.2) containing $CaCl_2$ (0.1 mM) and $MnCl_2$ (0.1 mM). The tested proteins include ConA, bovine serum albumin (BSA), thrombin (Thro), myoglobin (Myo), trypsin (Trp), cytochrome *c* (CytC), and lysozyme (Lys), which have the isoelectric point (p*I*) values of 4.7, 4.8, 7.1, 7.2, 10.5, 10.7, and 11, respectively. As shown in Figure 5, the yellow emission of **6** at 550 nm progressively increases at the expense of the blue emission of **P1** at 422 nm with increased ConA addition. The saturation occurs at [ConA] = 150 nM, where the yellow emission intensity is higher than that of the blue emission. The PL spectra of **6**/**P1** blend in the presence of nonspecific proteins with the same concentration (150 nM) are shown in Figure 6a. Different from ConA, nonspecific proteins almost do not enhance the acceptor emission, but change the donor emission differently. To quantitatively analyze the nonspecific interactions between protein and **6**/**P1** blend, the

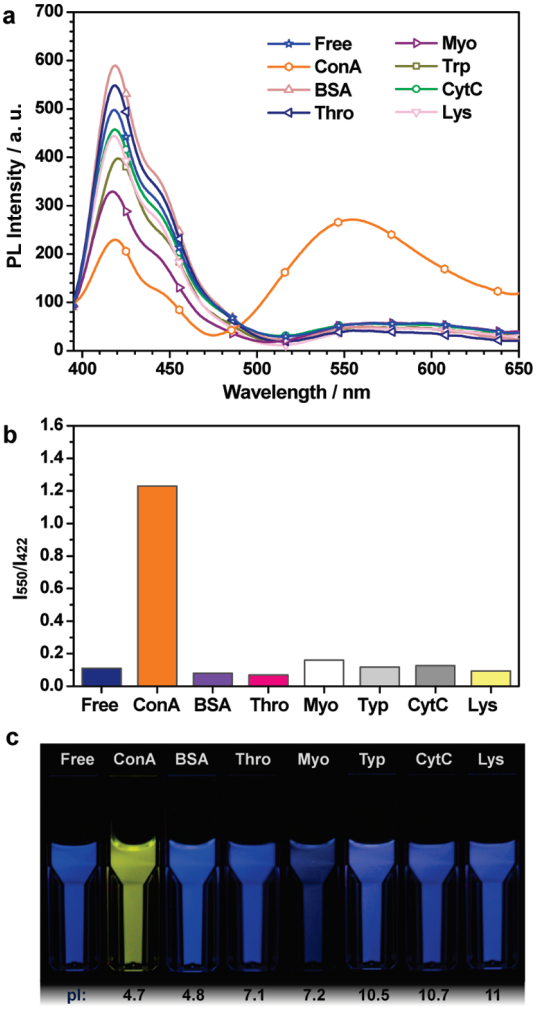

Figure 6. (a) PL spectra of **6**/**P1** blend in PBS (15 mM, pH = 7.2) containing $CaCl_2$ (0.1 mM) and $MnCl_2$ (0.1 mM) in the absence and presence of proteins. [**P1 RU**] = 1 μM, [**6**] = 0.5 μM and [protein] = 150 nM. Excitation at 370 nm. (b) The intensity ratio of the yellow emission of **6** at 550 nm to the blue emission of **P1** at 422 nm (I_{550}/I_{422}) as a function of proteins. The data are extracted from part a. (c) Photographs of the corresponding fluorescent solutions in part a under UV radiation at 365 nm.

intensity ratio of the yellow emission at 550 nm to the blue emission at 422 nm (I_{550}/I_{422}) for each protein is summarized in Figure 6b. It is obvious that only ConA shows $I_{550}/I_{422} > 1$, reflecting a high signal-to-noise ratio of **6**/**P1** blend for ConA sensing. The photographs of the corresponding fluorescent solutions of **6**/**P1** blend in the presence of different proteins are shown in Figure 6c. Because of the large I_{550}/I_{422}, the fluorescent color of **6**/**P1** blend turns into yellow in the presence of ConA, while it remains blue for other proteins. As a result, naked-eye discrimination of ConA from nonspecific proteins is feasible, which has not been realized so far for CPE based assays.

The distinguishable fluorescence signature of **P1**/**6** blend toward ConA from nonspecific proteins proves the protein-selective energy transfer from **P1** to **6**, which originates from specific binding between the mannose groups of **6** and ConA. The proposed mechanism is briefly illustrated in Scheme 4. ConA predominantly exists as a tetramer of four identical subunits in neutral or alkaline solutions, which has four binding sites for α-mannose units to bind in the presence of Ca^{2+} and Mn^{2+} ions.[19] In view of the high density of α-mannose substitutes for both **P1** and **6**, ConA can act as an

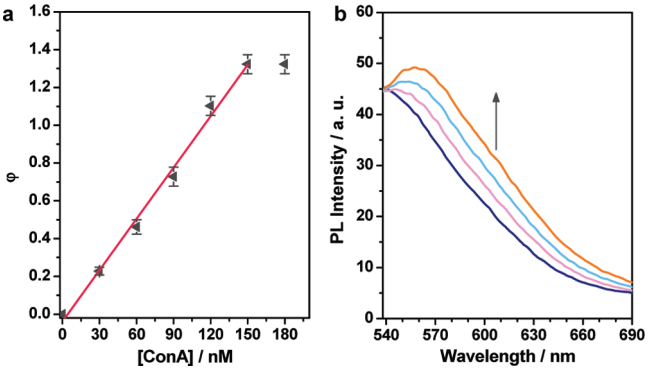

Figure 7. (a) φ as a function of [Con A] and its trendline. The data are based on the average of three independent experiments. (b) PL spectra of **6**/**P1** blend in PBS (15 mM, pH = 7.2) containing $CaCl_2$ (0.1 mM) and $MnCl_2$ (0.1 mM) in the absence and presence of Con A with the concentration ranging from 0 to 4.5 nM at intervals of 1.5 nM. [**P1 RU**] = 0.1 μM and [**6**] = 0.05 μM. Excitation at 370 nm.

Scheme 4. Schematic Illustration of Protein-Selective Energy Transfer from P1 to 6

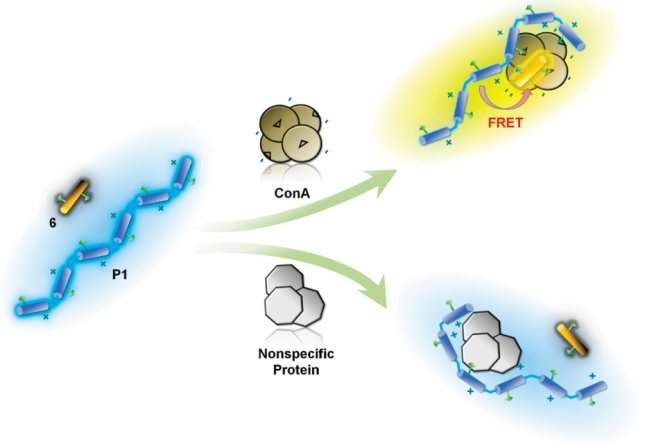

effective linker to bring **P1** and **6** into close proximity to form multicomponent complexes within which intermolecular contact increases to favor FRET (Scheme 4). In addition, as ConA (pI = 4.7) has net negative charges at pH = 7.2, electrostatic attraction between oppositely charged **P1** and ConA exists to tighten the complexes, which further promotes electronic coupling within the FRET pair. As a result of these combinational effects, efficient FRET from **P1** to **6** yields yellow fluorescence in the presence of Con A. Moreover, the presence of Ca^{2+} and Mn^{2+} ions in the detection medium provides a stronger yellow fluorescence response toward ConA for **6**/**P1** blend as compared to that in the absence of these metal ions (Figure S3 in the Supporting Information). This observation implies that the formation of ConA tetramer is beneficial to FRET between **P1** and **6** to afford a high signal-to-noise ratio.

On the contrary, nonspecific proteins do not have strong interactions with **6** which cannot substantially shorten the distance between **P1** and **6** to favor FRET (Scheme 4). However, the long aromatic backbone and positively charged side chains of **P1** make the hydrophobic and electrostatic interactions between **P1** and nonspecific proteins inevitable. Thereby, the emission of **P1** changes in the presence of nonspecific proteins depending on the charge and hydrophobicity of proteins. It is important to note that although Myo (pI = 7.2) has net neutral changes at pH = 7.2, it induces the most obvious intensity decrease in polymer emission among nonspecific proteins (Figure 6a). This is due to the metal center of Myo, which can quench the polymer fluorescence through charge transfer.[20] Nevertheless, the solution fluorescence of **6**/**P1** blend remains blue in the presence of nonspecific proteins (Figure 6c).

Protein Quantification. To demonstrate **6**/**P1** blend for ConA quantification, changes in the PL spectra in Figure 5 are correlated with ConA concentration. The calibration parameter φ is defined as the increment in I_{550}/I_{422} after addition of ConA.[21] Figure 7a shows φ as a function of [ConA] together with its trendline. The validity of ConA quantification using **6**/**P1** blend is verified by good overlap between the linear trendline and the original data in the range of 0 to 150 nM. The deviation from the trendline above 150 nM is caused by the saturation of yellow emission at 550 nm. To determine the limit of detection (LOD) for **6**/**P1** blend in Con A quantification, PL experiments were conducted with a diluted blend solution with [**P1 RU**] = 0.1 μM and [**6**] = 0.05 μM in PBS (15 mM, pH = 7.2) containing $CaCl_2$ (0.1 mM) and $MnCl_2$ (0.1 mM). As shown in Figure 7b, a progressive emission intensity increase is observed at 550 nm with ConA addition. Further decreasing the concentration of **6**/**P1** blend does not cause fluorescence enhancement at 550 nm in the presence of 1.5 nM ConA. These data reveal that the detectable complexation-induced FRET from **P1** to **6** occurs only when the analyte concentration is above 1.5 nM. As a result, the LOD for **6**/**P1** blend in ConA quantification is ~1.5 nM, which is significantly lower than that for mannose-substituted PF derivative based ConA assay.[16]

Conclusion

In conclusion, we synthesized a mannose-substituted cationic CPE (**P1**) and a mannose-substituted neutral conjugated oligomer (**6**) with blue and yellow emission, respectively. The spectral overlap between the polymer emission and the oligomer absorption enables us to blend them at an optimal molar ratio to form a sensitive bicomponent FRET probe. By virtue of the neutral and highly water-soluble nature of **6** and specific mannose/ConA binding, the distance between **P1** and **6** is substantially shortened in the presence of ConA instead of nonspecific proteins. As a consequence, **6**/**P1** blend exhibits efficient protein-selective FRET, allowing for label-free visual detection of ConA in a high-contrast and convenient manner. In addition, this FRET probe could be used to quantify ConA, providing a lower LOD (~1.5 nM) as compared to those for PF-based fluorescence quenching probes.

The findings shown in this work clearly highlight that incorporation of a neutral water-soluble conjugate oligomer as the energy acceptor in sensing operation and signal transduction minimizes the interference of CPE/protein nonspecific interactions, consequently offering a new strategy for highly selective protein sensing. This concept can be further generalized for multicolor detection of other proteins simply by attaching different recognition groups to the side chains, such as biotin for streptavidin. Moreover, facile modification of the backbone structures for both energy-donating CPE and energy-accepting conjugated oligomer allows one to adjust the signaling emission to any desirable wavelength for different tasks. As such, this study provides fundamental guidelines and new opportunities for CPE-based label-free chemical and biological sensing.

Experimental Section

Instruments. NMR spectra were collected on Bruker Avance 500 (DRX 500, 500 MHz). Matrix-assisted laser desorption/ionization time-of-flight (MALDI−TOF) was performed by

using 2,5-dihydroxybenzoic acid as the matrix under the reflector mode for data acquisition. Elemental analysis was performed on Perkin-Elmer 2400 CHN/CHNS and Eurovector EA3000 elemental analyzers. GPC analysis was conducted with a Waters 2690 liquid chromatography system equipped with a Waters 996 photodiode detector and a Waters 2420 evaporative light scattering detector using three Phenogel GPC columns in one loop. The molecular weight and polydispersity were obtained using polystyrenes as the standard and THF as the eluent at a flow rate of 1.0 mL/min at 35 °C. UV−vis absorption spectra were recorded on a Shimadzu UV-1700 spectrometer. PL measurements were performed on a Perkin-Elmer LS-55 equipped with a xenon lamp excitation source and a Hamamatsu (Japan) 928 PMT, using 90 deg angle detection for solution samples. The excitation energy at different wavelength was automatically adjusted to the same level by an excitation correction file. PL quantum yields were measured using quinine sulfate as the standard, with a quantum yield of 55% in H_2SO_4 (0.1 M). Fisher brand regenerated cellulose dialysis tubing with 1.5 kDa or 6.5 kDa molecular weight cutoff was used for dialysis. Freeze-drying was performed using Martin Christ Model Alpha 1−2/LD. Photographs of the fluorescent solutions were taken using a Canon EOS 500D Digital camera under a hand-held UV-lamp with λ_{max} = 365 nm. All PL and UV measurements were carried out at 24 ± 1 °C.

Materials. All proteins were purchased from Sigma-Aldrich Chemical Co. and were used as received. Ten × PBS buffer with pH = 7.4 (ultrapure grade) is a commercial product of first BASE Singapore. Milli-Q water (18.2 MΩ) was used to prepare the buffer solutions from the 10 × PBS stock buffer. Fresh stock solutions for **P1** (1 mM based on RU), **6** (1 mM) and proteins (0.1 mM) were prepared before use. NMR solvents, D_1-chloroform (99%) and D_4-methanol (99.5%), were purchased from Cambridge Isotope Laboratories, Inc. 2-Propynyl-2,3,4,6-tetra-*O*-acetyl-α-D-mannopyranose,[11g] 4,7-dibromobenzothiadiazole (**2**),[22] 2,7-dibromo-9,9-bis(6-bromohexyl)fluorene (**7**)[23] and 2-bromo-9,9-bis(2-(2-(2-bromoethoxy)ethoxy)ethyl)fluorene[24] were synthesized according to our previous reports. Other chemicals and biological reagents were purchased from Sigma-Aldrich Chemical Co., and were used as received.

Synthesis of 2-(9,9-Bis(2-(2-(2-bromoethoxy)ethoxy)ethyl)-fluorenyl)-4,4,5,5-tetramethyl-1,3,2-dioxaborolane (1). 2-Bromo-9,9-bis(2-(2-(2-bromoethoxy)ethoxy)ethyl)fluorene (3.18 g, 5 mmol), bis(pinacolato)diborane (1.5 g, 6 mmol), KOAc (1.75 g, 17.5 mmol), and anhydrous dioxane (50 mL) were mixed together. After degassing, [Pd(dppf)Cl_2] (0.125 g; dppf = 1,1′-bis(diphenylphosphanyl)ferrocene) was added. The reaction mixture was stirred at 90 °C overnight, and then cooled to room temperature. The organic solvent was removed, and the residual solid was dissolved in dichloromethane and washed with water. After drying with Na_2SO_4, the solvent was removed again. The crude product was purified by silica gel chromatography (hexane/ethyl acetate = 5:1) to give **1** as white crystals (2.89 g, 85%). ^{1}H NMR (500 MHz, $CDCl_3$, δ ppm): 7.85−7.77 (m, 2 H), 7.73−7.64 (m, 2 H), 7.48−7.38 (m, 1 H), 7.37−7.28 (m, 2 H), 3.65 (t, 4 H, *J* = 6.42 Hz), 3.42−3.30 (m, 8 H), 3.22−3.12 (m, 4 H), 2.83−2.62 (m, 4 H), 2.50−2.30 (m, 4 H), 1.38 (s, 12 H). ^{13}C NMR (125 MHz, $CDCl_3$, δ ppm): 149.40, 147.87, 143.33, 140.19, 134.07, 129.12, 127.83, 127.22, 123.13, 120.20, 119.08, 83.80, 71.03, 70.26, 69.83, 67.03, 51.05, 39.53, 30.08, 24.91. MS (MALDI−TOF): *m*/*z* 682.15 [M^+].

Synthesis of 4,7-Bis(9,9-bis(2-(2-(2-bromoethoxy)ethoxy)-ethyl)fluorenyl)benzothiadiazole (3). 1 (3.14 g, 4.60 mmol), 4,7-dibromobenzothiadiazole (**2**) (0.64 g, 2.2 mmol), $Pd(PPh_3)_4$ (53 mg, 0.046 mmol), and potassium carbonate (4.43 g, 32.0 mmol) were placed in a 100 mL round-bottom flask. A mixture of water (12 mL) and toluene (30 mL) was added to the flask, and the reaction vessel was degassed. The mixture was vigorously stirred at 90 °C for 2 days. After it was cooled to room temperature, dichloromethane was added to the reaction mixture. The organic portion was separated and washed with brine before drying over anhydrous Na_2SO4. The solvent was evaporated off, and the solid residues were purified by column chromatography on silica gel using hexane/ethyl acetate (1:3) to afford **3** as grassy yellow solid (1.9 g, 70%). ^{1}H NMR (500 MHz, $CDCl_3$, δ ppm): 8.13−8.02 (m, 4 H), 7.91 (s, 2 H),7.87 (2 H, d, *J* = 8.52 Hz), 7.77 (d, 2 H, *J* = 6.50 Hz), 7.48 (d, 2 H, *J* = 7.90), 7.38 (p, 2 H, *J* = 7.21, 7.19 Hz), 3.64 (t, 8 H, *J* = 6.41), 3.42 (dd, 8 H, *J* = 3.60, 5.70 Hz), 3.35 (t, 8 H, *J* = 6.41 Hz), 3.26 (dd, 8 H, *J* = 3.68, 5.50 Hz), 3.08−2.78 (m, 8 H), 2.65−2.35 (m, 8 H). ^{13}C NMR (125 MHz, $CDCl_3$, δ ppm): 154.25, 149.41, 149.34, 140.69, 140.06, 136.38, 133.31, 128.72, 127.99, 127.69, 127.45, 124.01, 123.24, 120.14, 119.91, 71.06, 70.35, 69.91, 67.28, 51.45, 39.68, 30.14. MS (MALDI−TOF): *m*/*z* 1244.15 [M^+]. Anal. Calcd for $C_{56}H_{64}Br_4N2O_8S$: C, 54.03; H, 5.18. Found: C, 54.12; H, 5.21.

Synthesis of 4,7-Bis(9,9-bis(2-(2-(2-azidoethoxy)ethoxy)ethyl)-fluorenyl)benzothiadiazole (4). 3 (0.88 g, 0.71 mmol), NaN_3 (0.23 g, 3.57 mmol), and DMF (4 mL) were placed in a 25 mL round-bottom flask. The reaction mixture was stirred at room temperature for 24 h and filtered to remove NaN_3 and NaBr. The filtrate was washed with water and extracted with CH_2Cl_2. The organic phase was separated and dried over Na_2SO4. After removal of the solvent, the residue was purified by silica gel column chromatography using hexane/ethyl acetate (1:3) as the eluent to afford **4** (0.71 g, 92%) as grassy yellow solid. ^{1}H NMR (500 MHz, $CDCl_3$, δ ppm): 8.15−8.04 (m, 4 H), 7.93 (s, 2 H),7.88 (2 H, d, *J* = 8.52 Hz), 7.78 (d, 2 H, *J* = 6.50 Hz), 7.50 (d, 2 H, *J* = 7.90), 7.40 (p, 2 H, *J* = 7.21, 7.19 Hz), 3.55 (t, 8 H, *J* = 6.41), 3.44 (dd, 8 H, *J* = 3.60, 5.70 Hz), 3.36 (t, 8 H, *J* = 6.41 Hz), 3.27 (dd, 8 H, *J* = 3.68, 5.50 Hz), 3.09−2.80 (m, 8 H), 2.67−2.37 (m, 8 H). ^{13}C NMR (125 MHz, $CDCl_3$, δ ppm): 154.28, 149.43, 149.35, 140.71, 140.10, 136.41, 133.33, 128.74, 128.00, 127.71, 127.48, 124.03, 123.26, 120.17, 119.94, 71.08, 70.37, 69.94, 67.31, 51.47, 50.40, 39.72.

Synthesis of 5. 2-Propynyl-2,3,4,6-tetra-*O*-acetyl-α-D-mannopyranose (1.31 mg, 3.4 mmol) and **4** (0.77 g, 0.7 mmol) were dissolved in THF (6 mL). An aqueous solution of sodium ascorbate (67 mg, 0.34 mmol) and copper(II) sulfate (27 mg, 0.17 mmol) was then added. The mixture was vigorously stirred at room temperature for 24 h, and then it was washed with water and extracted with CH_2Cl_2. The organic phase was separated and dried over Na_2SO_4. After removal of the solvent, the residue was purified by silica gel column chromatography using hexane/ethyl acetate (2:1) as the eluent to afford **5** (1.5 g, 82%) as grassy yellow solid. ^{1}H NMR (500 MHz, $CDCl_3$, δ ppm): 8.10−8.02 (m, 4 H), 7.90 (s, 2 H), 7.87 (d, 2 H, *J* = 7.88 Hz), 7.78 (d, 2 H, *J* = 6.80 Hz), 7.61 (s, 4 H), 7.49 (d, 2 H, *J* = 7.05 Hz), 7.43−7.33 (m, 4 H), 5.30 (m, 8 H), 5.21 (m, 4 H), 4.94 (s, 4 H), 4.78 (d, 4 H, *J* = 13.05 Hz), 4.62 (d, 4 H, *J* = 13.80 Hz), 4.42 (t, 8 H, *J* = 5.10 Hz), 4.28 (dd, 4 H, *J* = 4.92, 12.08 Hz), 4.15−4.00 (m, 8 H), 3.70 (t, 8 H, *J* = 5.18 Hz), 3.35 (m, 8 H), 3.21 (m, 8 H), 3.0−2.82 (m, 8 H), 2.58−2.38 (m, 8 H), 2.13 (s, 12 H), 2.10 (s, 12 H), 2.02 (s, 12 H), 1.96 (s, 12 H). ^{13}C NMR (125 MHz, $CDCl_3$, δ ppm): 170.65, 169.98, 169.82, 168.68, 154.26, 149.43, 143.18, 140.80, 140.10, 136.47, 133.30, 128.78, 128.00, 127.73, 127.56, 125.51, 124.08, 123.32, 120.21, 119.99, 96.82, 70.49, 69.85, 69.48, 69.27, 69.07, 68.69, 67.30, 66.11, 62.37, 60.87, 51.55, 50.20, 39.73, 20.86, 20.77, 20.68, 20.65. MS (MALDI−TOF): *m*/*z* 2638.70 [M^+].

Synthesis of 6. After **5** (500 mg, 0.19 mmol) was dissolved in the mixture of methanol (6 mL) and dichloromethane (10 mL), CH_3ONa in methanol solution (3 mL, 1 M) was added. The mixture was stirred at room temperature for 6 h. After rotary evaporation of the solvents, the residue was dissolved in water. Finally, the compound was purified by dialysis against Mill-Q water using a 1.5 kDa molecular weight cutoff dialysis membrane for 2 days. After freeze-drying, **6** (324 mg, 87%) was obtained as grassy yellow solid. ^{1}H NMR (500 MHz, CD_3OD, δ ppm): 8.22 (s, 2 H), 8.15−8.06 (m, 4 H), 8.01 (d, 2 H, *J* = 7.94 Hz), 7.96 (s, 4 H), 7.90 (d, 2 H, *J* = 7.98 Hz), 7.62 (d, 2 H, *J* = 6.53 Hz), 7.40 (p, 4 H, *J* = 7.10, 7.05 Hz), 4.70 (s, 4 H), 4.71−4.67 (m, 4 H), 4.62 (d, 4 H, *J* = 12.18 Hz), 4.51 (d, 4 H, *J* = 5.69 Hz), 4.38 (t, 8 H, *J* = 5.31 Hz), 3.75−3.60 (m, 12 H),

3.56 (br, 4 H), 3.50−3.33 (m, 12 H), 3.30−3.25 (m, 8 H), 3.17−3.09 (m, 8 H), 2.92−2.70 (m, 8 H), 2.48−2.30 (m, 8 H).

Synthesis of 9,9-Bis(2-(2-(2-azidoethoxy)ethoxy)ethyl)-2,7-dibromofluorene (8). 7 (1.52 g, 2.13 mmol), NaN_3 (0.69 g, 10.7 mmol), and DMF (10 mL) were placed in a 25 mL round-bottom flask. The reaction mixture was stirred at room temperature for 24 h and filtered to remove NaN_3 and NaBr. The filtrate was washed with water and extracted with CH_2Cl_2. The organic phase was separated and dried over Na_2SO4. After removal of the solvent, the residue was purified by silica gel column chromatography using hexane/dichloromethane (1:4) as the eluent to afford **8** (1.26 g, 93%) as white crystals. ^{1}H NMR (500 MHz, $CDCl_3$, δ ppm): 7.54 (s, 2 H), 7.51 (d, 2 H, J = 8.09 Hz), 7.47 (d, 2 H, J = 8.25 Hz), 3.54 (t, 4 H, J = 5.10 Hz), 3.38 (m, 4 H), 3.32 (t, 4 H, J = 5.07 Hz), 3.19 (m, 4 H), 2.80 (t, 4 H, J = 7.22 Hz), 2.34 (t, 4 H, J = 7.23 Hz). ^{13}C NMR (125 MHz, $CDCl_3$, δ ppm): 151.00, 138.50, 130.67, 126.76, 121.61, 121.24, 70.48, 70.07, 69.97, 66.89, 51.98, 50.60, 39.48.

Synthesis of 9. 2-Propynyl-2,3,4,6-tetra-*O*-acetyl-α-D-mannopyranose (1.31 mg, 3.4 mmol) and **8** (890 mg, 1.4 mmol) were dissolved in THF (6 mL). An aqueous solution of sodium ascorbate (67 mg, 0.34 mmol) and copper(II) sulfate (27 mg, 0.17 mmol) was then added. The mixture was vigorously stirred at room temperature for 24 h, and then it was washed with water and extracted with CH_2Cl_2. The organic phase was separated and dried over Na_2SO4. After removal of the solvent, the residue was purified by silica gel column chromatography using hexane/ethyl acetate (2:1) as the eluent to afford **9** (87%, 1.72 g) as colorless viscous liquid. ^{1}H NMR (500 MHz, $CDCl_3$, δ ppm): 7.64 (s, 2 H), 7.55 (s, 2 H), 7.52 (d, 2 H, J = 8.08 Hz), 7.47 (d, 2 H, J = 9.59 Hz), 5.30 (m, 4 H), 5.22 (s, 2 H), 4.94 (s, 2 H), 4.80 (d, 2 H, J = 12.26 Hz,), 4.65 (d, 2 H, J = 12.20 Hz,), 4.47 (t, 4 H, J = 5.11 Hz), 4.28 (dd, 2 H, J = 4.98, 12.24 Hz), 4.10 (m, 4 H), 3.73 (t, 4 H, J = 5.17 Hz), 3.32 (dd, 4 H, J = 3.69, 5.44 Hz), 3.14 (dd, 4 H, J = 3.90, 5.24 Hz), 2.80 (t, 4 H, J = 7.05 Hz), 2.33 (t, 4 H, J = 7.05 Hz), 2.13 (s, 6 H), 2.10 (s, 6 H), 2.02 (s, 6 H), 1.96 (s, 6 H). ^{13}C NMR (125 MHz, $CDCl_3$, δ ppm): 170.63, 169.95, 169.79, 169.66, 151.01, 143.20, 138.53, 130.66, 126.77, 124.06, 121.56, 121.28, 96.78, 70.39, 69.92, 69.45, 69.33, 69.04, 68.68, 66.90, 66.09, 62.36, 60.88, 52.10, 50.22, 39.44, 20.83, 20.75, 20.66, 20.63. MS (MALDI−TOF): m/z 1410.33 [M^+].

Synthesis of 2-(9,9-Bis(2-(2-(2-methoxyethoxy)ethoxy)ethyl)-7-(4,4,5,5-tetramethyl-1,3,2-dioxaborolan-2-yl)fluorenyl)-4,4,5,5-tetramethyl-1,3,2-dioxaborolane (10). 7 (3.55 g, 5 mmol), bis(pinacolato)diborane (3.0 g, 12 mmol), KOAc (3.5 g, 35 mmol), and anhydrous dioxane (50 mL) were mixed together. After degassing, [Pd(dppf)Cl_2] (0.25 g; dppf = 1,1′-bis(diphenylphosphanyl)ferrocene) was added. The reaction mixture was stirred at 90 °C overnight, and then cooled to room temperature. The organic solvent was distilled out, and the residual solid was dissolved in dichloromethane and washed with water. After drying with Na_2SO_4, the solvent was distilled out. The crude product was purified by silica gel chromatography using hexane/ethyl acetate (5:1) as the eluent to give **10** as white crystals (3.25 g, 80%). ^{1}H NMR (300 MHz, $CDCl_3$, δ): 7.89−7.70 (m, 4 H), 7.76−7.65 (m, 2 H), 3.66 (t, 4 H, J = 6.4 Hz), 3.38 (dd, 8 H, J = 5.8 Hz, J = 12.3 Hz), 3.16 (t, 4 H, J = 4.7), 2.69 (t, 4 H, J = 7.5 Hz), 2.44 (t, 4 H, J = 7.5 Hz), 1.39 (s, 24 H). ^{13}C NMR (75 MHz, $CDCl_3$ δ): 148.51, 143.11, 134.05, 129.21, 119.52, 83.84, 71.08, 70.31, 69.89, 67.00, 51.04, 39.47, 30.11, 24.93. MS (MALDI−TOF): m/z 808.25 [M^+]. Anal. Calcd for $C_{37}H_{54}B_2Br_2O_8$: C, 54.98; H, 6.73. Found: C, 55.17; H, 6.69.

Synthesis of P0. A Schlenk tube was charged with **9** (352 mg, 0.25 mmol), **10** (202 mg, 0.25 mmol), $Pd(PPh_3)_4$ (2.5 mg), and potassium carbonate (415 mg, 3.0 mmol) before it was sealed with a rubber septum. The Schlenk tube was degassed with three vacuum−argon cycles to remove air. Water (1.5 mL) and toluene (2.5 mL) were then added to the Schlenk tube and the mixture was frozen, evacuated, and thawed three times to further remove air. The polymerization was then carried out at 90 °C under vigorous stir for 12 h. The mixture was washed with water and extracted with $CHCl_3$. After the organic phase was separated, dried over $MgSO_4$ and concentrated, the residue was poured into methanol. The precipitate was filtered and then dried under vacuum for 24 h to afford **P0** (345 mg, 75%) as white fibers. ^{1}H NMR (500 MHz, $CDCl_3$, δ ppm): 8.14−7.31 (m, 14 H), 5.29 (m, 4 H), 5.22 (br, 4 H), 4.95 (s, 2 H), 4.79 (m, 2 H), 4.64 (m, 2 H), 4.46 (m, 4 H), 4.27 (m, 2 H), 4.07 (m, 4 H), 3.74 (m, 4 H), 3.64 (m, 4 H), 3.55−3.09 (m, 20 H), 3.02−2.76 (m, 8 H), 2.70−2.37 (m, 8 H), 2.15−1.91 (m, 24 H). ^{13}C NMR (125 MHz, $CDCl_3$, δ ppm): 170.67, 169.98, 169.83, 169.69, 150.12, 143.24, 143.18, 140.46, 139.55, 134.54, 134.02, 130.69, 130.54, 126.79, 124.04, 121.60, 121.53, 121.28, 120.45, 96.81, 83.91, 71.08, 70.50, 70.36, 70.04, 69.96, 69.49, 69.73, 69.08, 68.69, 67.31, 67.15, 66.13, 62.39, 60.90, 60.85, 50.57, 50.15, 39.93, 39.72, 30.31, 24.99, 20.86, 20.77, 20.68, 20.66.

Synthesis of P1. After **P0** (40.0 mg) was dissolved in the mixture of methanol (6 mL) and dichloromethane (10 mL), CH_3ONa in methanol solution (3 mL, 1 M) was added. The mixture was stirred at room temperature for 6 h for deacetylation. After rotary evaporation of the solvents, the residue was washed with water and ethanol, and dissolved in THF (8 mL). Condensed trimethylamine (∼2 mL) was added dropwise to the solution at −78 °C. The mixture was allowed to warm to room temperature. The precipitate was redissolved by the addition of methanol (10 mL). After the mixture was cooled to −78 °C, additional trimethylamine (∼2 mL) was added, and the mixture was stirred at room temperature for 24 h. After removal of the solvent, acetone was added. The precipitate was filtered and then dried under vacuum for 24 h to afford **P1** (36 mg, 82%) as white powders. ^{1}H NMR (500 MHz, CD_3OD, δ ppm): 8.36−7.48 (m, 14 H), 4.72 (s, 4 H), 4.68−4.58 (m, 4 H), 4.53−4.45 (m, 4 H), 4.43−4.32 (br, 8 H), 3.78−3.62 (br, 12 H), 3.56 (br, 4 H), 3.41 (br, 12 H), 3.23−3.09 (m, 8 H), 3.03 (m, ∼18 H), 2.80 (br, 8 H), 2.48−2.40 (br, 8 H).

Acknowledgment. The authors are grateful to the National University of Singapore (R-279-000-234-101, R279-000-301-646), Singapore Ministry of Education (R-279-000-255-112), and Ministry of Defense (R-279-000-301-232) for financial support. L.W. also thanks the China National Natural Science Foundation (20704043 & 21073221) for support. J.B. thanks National Natural Science Foundation of China (21004004) for financial support.

Supporting Information Available: Figues showing ^{1}H NMR and PL spectra. This material is available free of charge via the Internet at http://pubs.acs.org.

References and Notes

(1) (a) Kodadek, T. *Chem. Biol.* **2001**, *8*, 105–115. (b) Bunka, D. H. J.; Stockley, P. G. *Nat. Rev. Microbiol.* **2006**, *4*, 588–596.
(2) Wright, A. T.; Anslyn, E. V. *Chem. Soc. Rev.* **2006**, *35*, 14–28.
(3) (a) Thomas, S. W., III; Joly, G. D.; Swager, T. M. *Chem. Rev.* **2007**, *107*, 1339–1380. (b) Herland, A.; Inganäs, O. *Macromol. Rapid Commun.* **2007**, *28*, 1703–1713. (c) Nilsson, K. P. R.; Hammarström, P. *Adv. Mater.* **2008**, *20*, 2639–2645. (d) Feng, F. D.; He, F.; An, L. L.; Wang, S.; Li, Y. L.; Zhu, D. B. *Adv. Mater.* **2008**, *20*, 2959–2964. (e) Jiang, H.; Taranekar, P.; Reynolds, J. R.; Schanze, K. *Angew. Chem., Int. Ed.* **2009**, *48*, 4300–4316. (f) Lee, K. W.; Povlich, L. K.; Kim, J. S. *Analyst* **2010**, *135*, 2179–2189. (g) Li, K.; Liu, B. *Polym. Chem.* **2010**, *1*, 252–259.
(4) (a) Swager, T. M. *Acc. Chem. Res.* **1998**, *31*, 201–207. (b) Liu, B.; Bazan, G. C. *Chem. Mater.* **2004**, *16*, 4467–4476. (c) Bazan, G. C. *J. Org. Chem.* **2007**, *72*, 8615–8635. (d) Pu, K. Y.; Liu, B. *Biosens. Bioelectron.* **2009**, *24*, 1067–1073. (e) Pu, K. Y.; Liu, B. *J. Phys. Chem. B* **2010**, *114*, 3077–3084.
(5) (a) Kim, I. B.; Dunkhorst, A.; Bunz, U. H. F. *Langmuir* **2005**, *21*, 7985–7989. (b) Miranda, O. R.; You, C. C.; Phillips, R.; Kim, I. B.; Ghosh, P. S.; Bunz, U. H. F.; Rotello, V. M. *J. Am. Chem. Soc.* **2007**, *129*, 9856–9857.

(6) (a) Ho, H. A.; Leclerc, M. *J. Am. Chem. Soc.* **2004**, *126*, 1384–1387. (b) Béra Abérem, M.; Najari, A.; Ho, H. A.; Gravel, J. F.; Nobert, P.; Boudreau, D.; Leclerc, M. *Adv. Mater.* **2006**, *18*, 2703–2707. (c) Ho, H. A.; Najari, A.; Leclerc, M. *Acc. Chem. Res.* **2008**, *41*, 168–178.
(7) Li, H. P.; Bazan, G. C. *Adv. Mater.* **2009**, *21*, 964–967.
(8) (a) Wang, J.; Liu, B. *Chem. Commun.* **2009**, 2284–2286. (b) Zhu, Q.; Zhan, R. Y.; Liu, B. *Macromol. Rapid Commun.* **2010**, *31*, 1060–1064.
(9) (a) Gaylord, B. S.; Heeger, A. J.; Bazan, G. C. *Proc. Natl. Acad. Sci. U.S.A.* **2002**, *99*, 10954–10957. (b) Fan, C. H.; Plaxco, K. W.; Heeger, A. J. *Trends Biotechnol.* **2005**, *23*, 186–192. (c) Pu, K. Y.; Liu, B. *Adv. Funct. Mater.* **2009**, *19*, 1371–1378. (d) Pu, K. Y.; Zhan, R. Y.; Liu, B. *Macromol. Symp.* **2009**, *279*, 48–51. (e) Pu, K. Y.; Li, K.; Liu, B. *Adv. Mater.* **2010**, *22*, 643–646.
(10) Nimjee, S. M.; Rusconi, C. P.; Sullenger, B. A. *Annu. Rev. Med.* **2005**, *56*, 555–583.
(11) (a) Liu, B.; Bazan, G. C. *J. Am. Chem. Soc.* **2004**, *126*, 1942–1943. (b) Pu, K. Y.; Liu, B. *Macromolecules* **2008**, *41*, 6636–6640. (c) Yu, D.; Zhang, Y.; Liu, B. *Macromolecules* **2008**, *41*, 4003–4011. (d) Fang, Z.; Pu, K. Y.; Liu, B. *Macromolecules* **2008**, *41*, 8380–8387. (e) Dishari, S. K.; Pu, K. Y.; Liu, B. *Macromol. Rapid Commun.* **2009**, *30*, 1645–1650. (f) Shi, J. B.; Pu, K. Y.; Zhan, R. Y.; Liu, B. *Macromol. Chem. Phys.* **2009**, *210*, 1195–1200. (g) Shi, J. B.; Cai, L. P.; Pu, K. Y.; Liu, B. *Chem. Asian J.* **2010**, *5*, 301–308. (h) Pu, K. Y.; Zhan, R. Y.; Liu, B. *Chem. Commun.* **2010**, *46*, 1470–1472.
(12) (a) Schwartz, B. J. *Annu. Rev. Phys. Chem.* **2003**, *54*, 141–172. (b) Hennebicq, E.; Pourtois, G.; Scholes, G. D.; Herz, L. M.; Russell, D. M.; Silva, C.; Setayesh, S.; Grimsdale, A. C.; Müllen, K.; Brédas, J. L.; Beljonne, D. *J. Am. Soc. Chem.* **2005**, *127*, 4744–4762.
(13) (a) Heeger, P. S.; Heeger, A. J. *Proc. Natl. Acad. Sci. U.S.A.* **1999**, *96*, 12219–12221. (b) Dwight, S. J.; Gaylord, B. S.; Hong, J. W.; Bazan, G. C. *J. Am. Chem. Soc.* **2004**, *126*, 16850–16859.
(14) (a) Sharon, N.; Lis, H. *Science* **1972**, *177*, 949–959. (b) Dwek, R. A. *Chem. Rev.* **1996**, *96*, 683–720.
(15) Lis, H.; Sharon, N. *Chem. Rev.* **1998**, *98*, 637–674.
(16) (a) Disney, M. D.; Zheng, J.; Swager, T. M.; Seeberger, P. H. *J. Am. Chem. Soc.* **2004**, *126*, 13343–13346. (b) Xue, C. H.; Donuru, V. R. R.; Liu, H. Y. *Macromolecules* **2006**, *39*, 5747–5752. (c) Xue, C. H.; Jog, S. P.; Murthy, P.; Liu, H. Y. *Biomacromolecules* **2006**, *7*, 2470–2474. (d) Phillips, R. L.; Kim, I. B.; Tolbert, L. M.; Bunz, U. H. F. *J. Am. Chem. Soc.* **2008**, *130*, 6952–6954.
(17) (a) Liu, B.; Dishari, S. K. *Chem.—Eur. J.* **2008**, *14*, 7366–7375. (b) Pu, K. Y.; Fang, Z.; Liu, B. *Adv. Funct. Mater.* **2008**, *18*, 1321–1328.
(18) Liu, B.; Bazan, G. C. *J. Am. Chem. Soc.* **2006**, *128*, 1188–1196.
(19) Quiocho, F. A.; Reeke, G. N.; Beckert, J. W.; Lipscomb, W. N.; Edelmant, G. M. *Proc. Natl. Acad. Sci. U. S. A.* **1971**, *68*, 1853–1857.
(20) (a) Fan, C. H.; Plaxco, K. W.; Heeger, A. J. *J. Am. Chem. Soc.* **2002**, *124*, 5642–5643. (b) Zhang, Y.; Liu, B.; Cao, Y. *Chem. Asian J.* **2008**, *3*, 739–745. (c) Qin, A. J.; Lam, J. W. Y.; Tang, L.; Jim, C. K. W.; Zhao, H.; Sun, J. Z.; Tang, B. Z. *Macromolecules* **2009**, *42*, 1421–1424. (d) Li, Z.; Dong, Y. Q.; Lam, J. W. Y.; Sun, J. X.; Qin, A. J.; Häussler, M.; Dong, Y. P.; Sung, H. H. Y.; Williams, L. D.; Kwok, H. S.; Tang, B. Z. *Adv. Funct. Mater.* **2009**, *19*, 905–917.
(21) It results from subtraction of I_{550}/I_{422} in the absence of protein from that in the presence of ConA.
(22) Liu, B.; Bazan, G. C. *Nat. Protoc.* **2007**, *1*, 1698–1702.
(23) (a) Pu, K. Y.; Cai, L. P.; Liu, B. *Macromolecules* **2009**, *42*, 5933–5940. (b) Pu, K. Y.; Li, K.; Shi, J. B.; Liu, B. *Chem. Mater.* **2009**, *21*, 3816–3822.
(24) Pu, K. Y.; Liu, B. *Adv. Funct. Mater.* **2009**, *19*, 277–284.